Production of the grounds for melanoma classification using adaptive fuzzy inference neural network

Yuji Ikuma and Hitoshi Iyatomi
Department of Applied Informatics
Graduate school of Engineering, Hosei University
Tokyo Japan
iyatomi@hosei.ac.jp

***Abstract*—Several researchers investigated automated diagnosis for malignant melanomas as known as the worst skin cancer. Those systems, however, only provide final discrimination results but not related information such as their substantial reasons and therefore reliability of the system still remain an open issue. In this paper, we developed a new melanoma screening system based on an adaptive fuzzy inference neural network (AFINN). Our new system provides not only final discrimination result but also its grounds in easy-to-read fuzzy if-then format. Our system developed 88 fuzzy rules in consequence of the learning of 1148 dermoscopy images and in the classification, it provides both of the final result and its constituent rules. Based on only developed rules, our system achieved a sensitivity of 81.5% and a specificity of 73.9%. Since it is almost equivalent to expert dermatologists', we consider the developed rules are reasonable and this supplemental information improves overall system reliability.**

***Index Terms*—dermoscopy, melanoma, fuzzy neural network**

I. Introduction

Malignant melanoma is the worst skin cancer. If patients have an advanced melanoma, their five-year survival rate is reported as around 10% [1]. While, on the other hand, early-stage melanoma can be cured in many cases, particularly before the metastasis phase. For example, patients with a melanoma less than or equal to 0.75 mm in thickness have a good prognosis and their five-year survival rate is greater than 93% [2]. Therefore, early detection is crucial for the reduction of melanoma-related deaths. However, discrimination between early stage melanomas and nevi is often difficult even by expert dermatologists.

Dermoscopy [3], a non-invasive skin imaging technique, and diagnosis scheme using it, such as the ABCD rule [4] and the 7-point checklist [5] were introduced to improve the diagnostic accuracy. However, dermoscopic diagnosis is often subjective and is therefore associated with poor reproducibility and low accuracy especially in the hands of inexperienced dermatologists. Despite the use of dermoscopy, the accuracy of expert dermatologists in diagnosing melanoma is estimated to be about 75-84% [6], [7].

In such backgrounds, automated analysis techniques to overcome above mentioned problems have been reported [8]-[16]. Table I summarizes some typical preceding studies. Note that each of them was established based on different dataset and therefore diagnosis accuracy cannot be compared simply. Rubegni et al. [8] achieved a sensitivity (SE: melanoma detection accuracy) of 94.3% and a specificity (SP: nevus detection accuracy) of 93.8% on 350 cases of nevi and 200 cases of melanoma using an artificial neural network (ANN) with 48 image features. Celebi et al. [13] selected 18 image features from 476 cases of nevi and 88 cases of melanomas and developed a support vector machine classification model with a radial basis function (RBF) kernel. Their classifier achieved a SE of 93.3% and a SP of 92.3%. Tenenhaus et al. [15] analyzed 195 cases of nevi and 32 cases of melanomas and achieved SE of 95% and SP of 60% based on only three image features using the kernel logistic partial least square regression technique. Similarly, Zho et al. [16] achieved SE of 82.1% and SP of 86.3% based on only 4 symmetrical image features. For the past almost ten years we have been developing an Internet-based melanoma screening system [10] (available at http://dermoscopy.k.hosei.ac.jp) Using an Internet connection anyone who has a dermoscopy image can use our screening system from anywhere in the world. The latest version of our system achieved 85.9% of SE and 86.0% of SP on a set of 1258 non-acral dermoscopy images (1060 melanocytic nevi and 198 melanomas) [14] and 93.3% in SE, 91.1% in SP on a set of acral volar 199 dermoscopy images (169 melanocytic nevi and 30 melanomas) [17] using an ANN and linear classifier, respectively.

Although some of these automated techniques showed superior classification performance to expert dermatologists on a simple numerical evaluation, those techniques cannot supersede physicians in current situation due to several reasons. The primary cause is associated with the system reliability. Most of conventional systems have developed based on limited number of images (see Table I) because it is usually difficult for researchers to prepare large dataset with established diagnosis. From an another point of view, present automated systems only provide final discrimination results but not related information such as their substantial reasons, degree of confidence etc.

978-1-4799-0652-9/13 $31.00 © 2013 IEEE
DOI 10.1109/SMC.2013.439

TABLE I
COMPARISON OF CLASSIFICATION PERFORMANCE OF PRECEDING STUDIES

	[8]	[9]	[10]*	[11]	[12]	[13]	[14]*	[15]	[16]
Year	2002	2004	2004	2005	2005	2007	2008	2010	2012
Author	Rubegni et al	Blum et al	Oka et al	Seidenari et al	Menzies et al	Celebi et al	Iyatomi et al	Tenenhaus et al	Zho et al
SE (%)	94.3	83.3	87.0	87.5	91	92.3	85.9	95	82.1
SP (%)	93.8	86.9	93.1	85.7	65	93.3	86.0	60	86.3
classifier	ANN	Logistics	Linear	Linear	Logistics	SVM	ANN	KL-PLS	SVM
# melanomas	217	84	77	95	382	88	198	32	88
# nevi	371	753	188	364	2048	476	1060	195	263

* available via Internet (http://dermoscopy.k.hosei.ac.jp)

Since target users of current systems are inexperienced dermatologists or physicians with other expertise, they need detailed information that support their decision, i.e. diagnosis.

In the meantime, fuzzy neural networks (FNNs) such as ANFIS [18] combines both advantages of the fuzzy systems and the learning ability of the neural network. These techniques alleviate the issues of fuzzy modeling by means of the learning ability of neural networks. More concretely, FNNs develop fuzzy if-then rules automatically during their training phase and make an inference based on these rules.

In this study, we developed a new melanoma screening system based on a adaptive fuzzy inference neural network (AFINN) [19]. AFINN has a simple structure and capability of high dimensional data. In the learning phase of AFINN, it develops fuzzy if-then rules relevant to melanoma discrimination automatically. When our system receives the test dermoscopy image in practical usage, the system presents not only classification result but also applied fuzzy if-then rules to yield the result as the grounds for "diagnosis".

II. MATERIAL AND METHOD

Fig.1 shows the schematics of our new melanoma screening system. Our system consists of following four components: (i) tumor area segmentation, (ii) feature extraction, (iii) feature selection, and (iv) AFINN. From an operation view, our system has two phases: (1) training phase and (2) classification phase.

In the training phase, image features for training were extracted from each training dermoscopy image using the components (i)-(iii) and AFINN develops fuzzy if-then rules for melanoma classification based on them in (iv).

In the classification phase, tumor area of the test dermoscopy image is segmented out by the component (i) and then only requisite image features were extracted (ii)-(iii) and finally, AFINN performs a fuzzy inference with only the fuzzy rules developed in the training phase (iv). In the following subsections, we explain each step briefly.

A. Material

In this study, we used a total of 1148 dermoscopy images contained 980 benign nevi and 168 melanomas. The breakdown is followings. 1) 188 Clerk nevi, 56 Reed nevi, 75 melanomas including 23 melanomas *in situ* from Universities of Naples and Graz. 2) 288 nevi and 15 melanomas from Keio University. 3) 448 nevi and 78 melanomas from University of Vienna. These results were determined by a pathological examination or agree of diagnosis by several dermatologists.

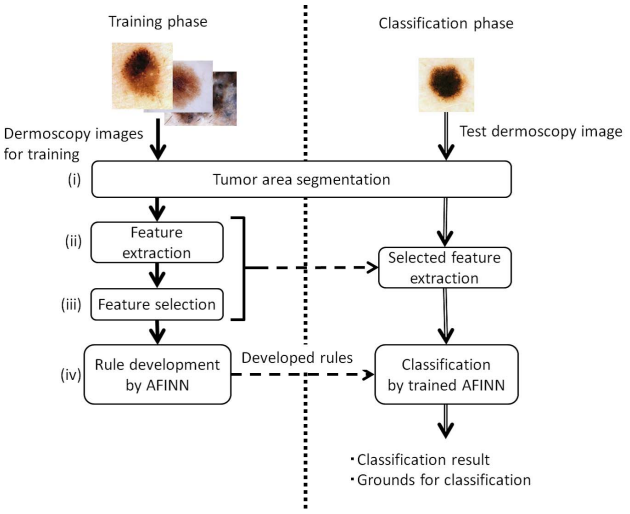

Fig. 1. Schematics of our melanoma screening system.

B. Tumor area segmentation

The accuracy of diagnosis for a tumor depends greatly on the accurate extraction of the tumor area. We extracted the tumor area using our "dermatologist-like" tumor extraction algorithm [20] that combines both pixel-based and region-based methods and utilizes a region-growing method that aims to bring the automatic extraction results closer to those determined by dermatologists. The segmentation algorithm comprises four phases: (1) initial tumor area decision, (2) regionalization, (3) tumor area selection, and (4) region-growing. In our previous research, we confirmed the algorithm to be highly accurate in that the extracted areas were almost equivalent to those determined by dermatologists.

C. Feature extraction

After tumor areas were determined, we extracted a total of 282 features from tumor body, periphery, and associated surrounding normal skin. Those are categorized into color, border, symmetry and texture with reference to diagnosis schema used in clinical. We present those breakdowns in follows.

1) Color-related features: As color-related features, a total of 140 parameters were calculated: minimum (min), average (ave), maximum (max), standard deviation (S.D.), and

skewness (skw) values in the RGB and HSV color spaces, respectively for the tumor area (T), periphery of tumor area (P), difference between the surrounding normal skin and tumor area (S-T), and difference between the surrounding normal skin and periphery of tumor area (S-P), (subtotal: $5 \times 6 \times 4 = 120$ features). In addition, (i) the average color of surrounding skin, (ii) average color difference between the peripheral and inside of the tumor in the RGB and HSV color channels, respectively (subtotal: $6 \times 2 = 12$), and (iii) the number of colors ($\#C$) in the tumor and its peripheral area in the RGB and HSV color spaces quantized into 8^3 and 16^3 colors, respectively as a polychrome features (subtotal:$2 \times 2 \times 2 = 8$) were calculated. Note that the peripheral part of tumor is defined as the region of the border that has an area equal to 30% of the tumor area as determined by a recursive dilation process applied to the outer border, working inward from the border of the extracted tumor.

2) Border-related features: As border-related features, a total of 4 parameters were calculated. The tumor area was divided into eight equi-angle regions. In each region, the ratio of the color intensity inside and outside of the tumor and the gradient of intensity were calculated in the blue and luminance channels ($ratio_b, ratio_l, grad_b, grad_l$) respectively.

3) Symmetry-related features: A symmetry-related features, a total of 26 parameters were calculated. We designed 6 intensity threshold values δ from 100 to 250 with a stepsize of 30. In the extracted tumor area, thresholding was performed and the areas whose intensity was lower than the threshold were determined. From each such area, we calculated 8 features: area ratio to the original tumor size ($area^\delta$), circularity ($circ^\delta$), differences of the center of gravity between original tumor ($\Delta_x^\delta, \Delta_y^\delta$), standard deviation of the distribution ($\sigma_x^\delta, \sigma_y^\delta$)

4) Texture-related features: As texture-related features, a total of 112 parameters were calculated. We prepared 7 co-occurrence matrices with distance value ranging from 1/4 to 1/32 of the major axis of tumor object with a step ratio of $\sqrt{2}$. Based on each co-occurrence matrix, energy, moment, entropy, and correlation were calculated in four directions (0, 45, 90 and 135 degree).

D. Feature selection

Feature selection is very important in terms of robustness of the classification, readability of the created if-then rules, calculation cost and so on. Since a classifier having high correlation parameters brings on serious problems so called multi-collinearity, we firstly investigated correlation between every possible combinations of two parameters and deleted one of them where their correlation higher than the threshold ξ . We repeated this procedure until correlation between any two parameters were less than ξ .

Considering the classification boundary shape of the classifier is also important for feature selection. AFINN develops ellipse hyperplanes as classification boundaries, similar to the one developed by a support vector machine (SVM) [21] classifier with the radial basis function kernel. In this study, therefore, we used feature selection method used in SVM

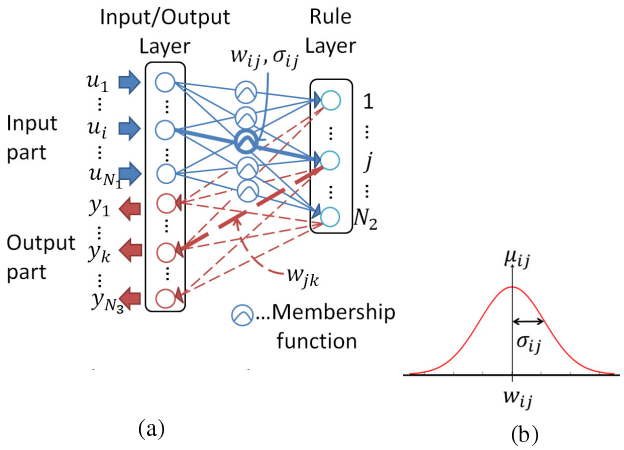

Fig. 2. (a) Structure of AFINN and (b) its membership function.

model [22]. SVM satisfies both of high classification accuracy and calculation speed by means of kernel trick which maps input data space to higher dimensional space. The shortest distance between classification boundary and its constituent data points (i.e. support vectors) is called as the margin and the classifier with larger margin is generally considered as more reliable and robust over impediments. Therefore this feature selection method stands on the idea that if tentative elimination of arbitrary feature shows little impact on the margin size, the feature makes little influence for the classification and therefore can be eliminated. In this study, we firstly developed SVM with all image features (after elimination of highly correlated features) and deleted features one by one using following scheme. In each elimination step, each feature is temporarily eliminated by rotation and its impact for the margin of the classification boundary is investigated. If the image feature has the smallest impact on the margin among tested features and is less than the threshold $\theta_{svm} = 0.2$, we regard this feature as not important and therefore eliminated.

Repeat this elimination step until the number of the features becomes constant. Finally, we trained AFINN with remaining features.

E. Adaptive fuzzy inference neural network

1) Structure of AFINN: Fig. 2 shows the structure of AFINN. It consists of two layers. One is the input-output (I/O) layer and another is the rule-layer. The I/O layer consists of the input-part and the output-part. Each node in the rule-layer represents one fuzzy rule. Weights from the input-part to the rule-layer and those from the rule-layer to the output-part are fully connected and they store fuzzy if-then rules. Membership functions as premise part are expressed in the weights. Each weight from the rule-layer to the output-part corresponds to the estimated value of each rule. In short, the weights from the input-part to the rule-layer indicate if-parts of fuzzy if-then rules and those from the rule-layer to the output-part indicate then-parts. The shapes of membership functions are adjusted automatically in the learning phase.

2) Behavior of AFINN: Suppose that the number of neurons in the input-part, which is equal to the dimension of the input data, is N_1, the number of rules is N_2, and the number of neurons in the output-part, which is equal to the dimension of the output data, is N_3. The input data to the AFINN is expressed as follows:

$$\boldsymbol{U} = \{u_1, u_2, ..., u_i, ..., u_{N_1}\}. \quad (1)$$

The subscripts i, j, and k refer to the nodes in the input part, those in the rule-layer, and those in the output-part, respectively. Fig. 2(b) shows an example of a membership function. The bell-shaped membership function represents the if-part of fuzzy rule, which is placed between the ith input node and the jth node in the rule-layer. The membership function is expressed as

$$\mu_{ij} = \exp\left(-\frac{(u_i - w_{ij})^2}{\sigma_{ij}^2}\right), i = (1, 2, ..., N_1), j = (1, 2, ..., N_2) \quad (2)$$

where μ_{ij} is the membership value, w_{ij} and σ_{ij} are the center and width of the membership function respectively, and are adjusted using the steepest descent method in the parameter estimation phase.

In the rule-layer, AFINN calculates the degree of the rule as follows:

$$\rho_j = \prod_i^{N_1} \mu_{ij}^{1/N_{adj}}. \quad (3)$$

Here, N_{adj} is the compensated factor in attempt to high dimensional data. Then, the inference result of the kth node in the output part is calculated by the following equation:

$$\hat{y_k} = \frac{\sum_j^{N_2}(w_{jk}\rho_j)}{\sum_j^{N_2}\rho_j}, k = (1, 2, ..., N_3) \quad (4)$$

where w_{jk} is the weight between the jth node in the rule layer and the kth node in the output-part. The w_{jk} corresponds to the estimated value of the jth rule for the kth node in the output-part. The logical form of the jth fuzzy if-then rules is given such as

if u_1 is μ_{1j} and u_2 is μ_{2j} and ... u_{N_1} is $\mu_{N_1 j}$
then y_k is w_{jk}.

3) Learning of AFINN: AFINN adjusts parameters such as $w_{ij}, \sigma_{ij}, w_{jk}$ using the steepest descent method and it derives fuzzy if-then rules automatically. Please refer original article [19] in detail. In this study, input vector $\boldsymbol{U}$ consists of image parameters extracted and selected from dermoscopy images and output vector $\boldsymbol{Y}$ is scalar value (this time $N_3 = 1$) and assigned as 0 or 1 for benign or malignant cases, respectively.

III. Results

A. Feature selection

Elimination of highly correlated image features with threshold ξ reduced the number of features to 109 from the original 282. Note that we determined $\xi = 0.9$ by preliminary experiments.

TABLE II
SELECTED FEATURES

No.	Description	Addr.
1	Minimum green value inside the tumor	$\min_g^T$
2	Minimum red value in the periphery	$\min_r^P$
3	Minimum difference of green value between skin and tumor	$\min_g^{S-T}$
4	Maximum red value inside the tumor	$\max_r^T$
5	Standard deviation of red value inside the tumor	S.D.$_r^T$
6	Standard deviation of saturation value inside the tumor	S.D.$_s^T$
7	Skewness of hue value inside the tumor	skw$_h^T$
8	Skewness of blue value in the periphery	skw$_b^P$
9	Area ratio between original tumor and tumor brightness 130 or less	area^{130}

The following feature selection strategy based on the investigation of margin of SVM classifier [22] selected 9 image features. Table II summarizes the selected 9 features with the selected order. Note here that abbreviation $\min_g^T$ presents minimum green (g) value inside the tumor (T).

B. Training of AFINN and developed fuzzy rules

A total of 88 fuzzy if-then rules were developed as a result of the training phase of our system. Table III shows examples of those developed rules. In each column, ID represents serial number of rules, following 9 values are central value of fuzzy membership function associated with related features (i.e. former part of fuzzy rules, w_{ij}), and the most right column indicates the classification value (i.e. latter part of fuzzy rules; w_{jk}) such as benign (0) or malignant (1).

The modeling and learning parameters are summarized in Table IV. Those were determined based on preliminary experiments. Here ξ_{SELF} is threshold for integration of similar rules in the rule creation phase, α is the weight factor of input data space, $\epsilon_{SELF_{init}}$ is the initial value of learning constant of rule creation phase, E_{finish} is the lower limit of training error determines continuation of the training, ϵ_{LMS} is the learning constant in the LMS (least mean square) learning phase and σ_{init} is initial value of σ_{ij}. Please refer original manuscript in detail [19].

C. Classification of melanomas and its ground

The trained AFINN performed a fuzzy inference based on only developed 88 rules and it achieved the classification accuracy of 81.5% in SE and 73.9% in SP under the leave-one-out cross validation. Note that providing this result is not intended to insist on classification performance, but validity of the developed rules. Fig.3 shows three dermoscopy images as test examples. Table V summarized the extracted image features, the top three fuzzy rules lead to the final result, its relative degree of fitness ($\rho_j / \sum \rho$), the final output of AFINN and its interpretation (i.e. classification result) corresponds to each image in Fig.3.

IV. Discussion

A. Interpretation of developed rules

We discuss developed fuzzy rules with in Table III. The 14-th rule (rule for benign nevi: latter part is 0.0) has quite larger $\min_g^T$ (minimum green value inside the tumor) value than

TABLE III
DEVELOPED RULES

	If (former part)									then
ID	$\min_g^T$	$\min_r^P$	$\min_g^{S-T}$	$\max_r^T$	S.D.$_r^T$	S.D.$_s^T$	skw_h^T	skw_b^P	area^{130}	classification*
14	111.94	200.81	-23.60	255.01	11.32	0.13	49.45	-0.23	0.02	0.00
17	25.75	98.47	18.19	230.67	34.34	0.02	-22.57	-0.70	0.83	0.00
22	-5.36	-37.69	-13.94	254.42	74.95	0.23	-1.40	-0.91	0.77	0.99
25	0.02	103.92	-80.92	255.01	57.45	0.09	88.92	-0.07	0.85	1.00
29	-3.37	-22.19	-11.29	257.62	65.81	0.24	5.85	-0.21	0.81	0.01
42	15.96	84.51	-83.88	212.35	44.12	0.05	-11.08	-0.49	0.69	0.00
54	8.65	107.39	-10.39	146.77	17.75	0.23	11.36	-0.59	0.69	0.99
69	24.05	156.84	-33.68	254.17	37.31	0.20	3.34	0.88	0.86	0.00
79	0.63	-21.77	-32.56	186.65	44.10	0.20	9.76	-0.33	1.09	0.95
88	8.03	47.79	-143.98	255.01	31.37	0.12	1.02	0.60	0.00	1.00

* Consequent part of the fuzzy rule [0,1] (0:benign 1:malignant)

TABLE IV
MODELING AND LEARNING PARAMETERS OF AFINN

N_1	N_3	ξ_{SELF}	α	$\epsilon_{SELF_{init}}$	N_{adj}	E_{finish}	ϵ_{LMS}	σ_{init}
9	1	0.7	0.25	0.05	$N_1/2$	0.03	0.001	0.1

(a) nevus

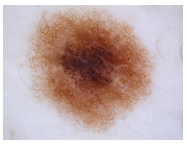

(b) nevus

(c) melanoma

Fig. 3. Test example of dermoscopy images.

TABLE V
EXECUTION EXAMPLES FOR IMAGES SHOWN IN FIG.3

		if (former part)										then*	rule fitness	final result
image		No	$\min_g^T$	$\min_r^P$	$\min_g^{S-T}$	$\max_r^T$	S.D.$_r^T$	S.D.$_s^T$	skw_h^T	skw_b^P	area^{130}		$\rho_j / \sum \rho(\%)$	
Fig.3.(a)	Extracted feature		11	124	-8	255	84.44	0.19	18.10	-0.76	0.63	n/a		0.01 nevus
	Rules:1	2	11.00	132.25	1.96	259.25	105.00	0.20	25.32	-0.86	0.62	0.01	99.9	
	Rules:2	18	3.44	203.64	-4.88	259.45	76.92	0.20	17.78	-0.38	0.64	0.99	0.00	
	Rules:3	76	0.52	12.85	-33.17	196.33	43.00	0.16	7.72	-0.27	0.75	0.19	0.00	
Fig.3.(b)	Extracted feature		47	117	-7	253	37.59	0.13	-1.11	-0.18	0.68	n/a		-0.00 nevus
	Rules:1	38	74.41	89.13	2.65	235.61	71.17	0.11	1.40	-0.16	0.52	0.00	94.3	
	Rules:2	65	1.71	1.04	-18.77	259.91	14.99	0.08	-0.12	-1.81	0.99	0.00	2.5	
	Rules:3	76	0.52	12.85	-33.17	196.33	43.00	0.16	7.72	-0.27	0.75	0.19	2.0	
Fig.3.(c)	Extracted feature		4	154	-17	255	67.00	0.19	13.25	-0.37	0.65	n/a		0.96 melanoma
	Rules:1	18	3.44	203.64	-4.88	259.45	76.92	0.20	17.78	-0.38	0.64	0.99	97.0	
	Rules:2	29	-3.37	-22.19	-11.29	257.62	65.81	0.24	5.85	-0.21	0.81	0.01	0.07	
	Rules:3	44	27.99	97.02	-15.98	180.91	31.37	0.21	0.64	-3.41	0.70	0.00	0.06	

* Consequent part of the fuzzy rule [0,1] (0:benign 1:malignant)

others. Since green channel correlates strongly with intensity or luminance channel, the larger this value indicates the brighter the inside of tumor. This suggests that the difference in intensity between tumor and surrounding healthy skin is not large, can be interpreted as border of the tumor is relatively ambiguous. This fact corresponds with a category B (Border) of the ABCD rule [4] indicates that the tumor with clear boundary tends to be melanomas.

In other example, the 79-th rule (rule for malignant melanomas: latter part is 0.95), area^{130}(ratio of dark area to original tumor size) is larger than others. This fact suggests that the lesion has large dark region and therefore has a relatively clear border. This case is also applicable to an example of category B in the ABCD rule.

Fuzzy if-then rules created by AFINN likes above have a lot of commons with clinical findings used in practice. There are some exceptions typically for images with blue-white structures (inside of the tumor seems blue, gray and/or white in color due to existence melanin cells in deeper skin area or effect of regression structure). We consider that it is mainly

due to the tumor extraction algorithm used in this study did not extract those area appropriately.

B. Evaluation of developed rules and classification accuracy

AFINN yields final results using a fuzzy inference only with the developed fuzzy rules. In this study, our trained AFINN achieved the classification accuracy of 81.5% in SE and 73.9% in SP as previously described. From only the numerical point of view, this result is rather lower to conventional models shown in Table I, which pursue only accuracy. However, our result is still equivalent to diagnosis accuracy of skilled dermatologist (75-84%) and therefore the developed fuzzy if-then rules were considered as reasonable.

The objective of this study is to provide the user the "grounds for diagnosis". We have a confident that providing fuzzy rules lead to the classification result must be its easy-to-read grounds and therefore they help the users (i.e. physicians) to make their "diagnosis".

From an analytical view, since fuzzy neural networks, including AFINN lay weight on a readability of the input-output data space (i.e. fuzzy if-then rules), degrees of freedom of the system is restricted in comparison with the same scale multilayer neural networks or similar non-linear models and therefore they are at disadvantage in the "numerical" classification accuracy in many cases. The outcome of above discussions, we conclude that we should better to improve overall system reliability by providing both results; (1) accuracy oriented final classification result calculates by conventional classifiers, and (2) reliability oriented grounds for the classification.

V. Conclusion

The objective of this study is to build the melanoma classification system to have a capability of providing not only results but also its grounds in easy-to-read format. In this paper, we applied the adaptive fuzzy inference neural network (AFINN). The trained AFINN achieved a sensitivity of 81.5% and a specificity of 73.9% based on only developed 88 fuzzy rules under the leave-one-out cross validation. AFINN also provides the grounds for final classification result in fuzzy if-then format and it should improve the overall system reliability. We are planning to implement this model on our Internet-based automated melanoma screening system in the near future.

Acknowledgment

This research was partially supported by the Ministry of Education, Culture, Science and Technology of Japan (Grant-in-Aid for Young Scientists program (B), 23791295, 2011-2012).

References

[1] Center for Cancer Control and Information Services, National Cancer Center, Japan (http://ganjoho.jp)

[2] F.L.Meyskens.Jr, D.H.Berdeaux, B.Parks, T.Tong, L.Loescher, T.E.Moon, "Natural history and prognostic factors influencing survival in patients with stage I disease," Cancer, Vol. 62, No. 6, pp.1207-1214, 1998.

[3] H.P.Soyer, J.Smolle, H.Kerl, H.Stettner, "Early diagnosis of malignant melanoma by surface microscopy," Lancet, Vol. 2, p.803, 1987.

[4] W.Stolz, A.Riemann, A.B.Cognetta, L.Pillet, W.Abmayr, D.Holzel, et al., "ABCD rule of dermatoscopy:a new practical method for early recognition of malignant melanoma," European Journal of Dermatology, Vol. 4, No. 7, pp.521-527, 1994.

[5] G.Argenziano, G.Fabbrocini, P.Carli, V.D.Giorgi, et al., "Epiluminescence microscopy for the diagnosis of doubtful melanocytic skin lesions comparison of the ABCD Rule of Dermatoscopy and a New 7-Point Checklist Based on Pattern Analysis," Arch Dermatol, Vol. 134, No. 12, pp.1563-1570, 1998.

[6] W.Stolz, O.B.Falco, P.Bliek, M.Kandthaler, W.H.C.Burgdorf, A.B.Cognetta, "Color atlas of dermatoscopy," 2nd enlarged and completely revised edition, Berlin: Blackwell publishing, 2002.

[7] G.Argenziano, H.P.Soyer, S.Chimenti, R.Talamini, R.Corona, F.Sara, et al., "Dermoscopy of pigmented skin lesions: results of a consensus meeting via the Internet," Journal of American Academy of Dermatology, Vol. 48, No. 5, pp.679-693, 2003.

[8] P.Rubegni, G.Cecenini, M.Burroni, R.Perotti, G.Del'Eva,P.Sbano, et al., "Automated diagnosis of pigmented skin lesions," International Journal of Cancer, Vol. 101, No. 6, pp.576-580, 2002.

[9] A.Blum, H.Luedtke, U.Ellwanger, R.Schwabe, G.Rassner, C.Garbe, "Digital image analysis for diagnosis of cutaneous melanoma. Development of a highly effective computer algorithm based on analysis of 837 melanocytic lesions," British Journal of Dermatology, Vol. 151, No. 5, pp.1029-1038, 2004.

[10] H.Oka, M.Hashimoto, H.Iyatomi, G.Argenziano, H.P.Soyer, M.Tanaka, "Internet-based program for automatic discrimination of dermoscopic images between melanomas and Clark naevi," British Journal of Dermatology, Vol. 150, No. 5, p.1041, 2004.

[11] S.Seidenari, G.Pellacani, C.Grana, "Pigment distribution in melanocytic lesion images: a digital parameter to be employed for computer-aided diagnosis," Skin Research and Technology, Vol. 11, No. 4, pp.236-241, 2005.

[12] S.W.Menzies, L.Bischof, H.Talbot, A.Gutenev, M.Avramidis, L.Wong, et al., "The performance of Solar Scan an automated dermoscopy image analysis instrument for the diagnosis of primary melanoma," Archives of dermatology, Vol. 141, No. 11, pp.1388-1396, 2005.

[13] M.E.Celebi, H.A.Kingravi, B.Uddin, H.Iyatomi, et al., "A methodological approach to the classification of dermoscopy images," Computerized Medical Imaging and Graphics, Vol. 31, No. 6, pp.362-373, 2007.

[14] H.Iyatomi, H.Oka, M.E.Celebi, M.Hashimoto, M.Hagiwara, M.Tanaka, K.Ogawa, "An improved Internet-based melanoma screening system with dermatologist-like tumor area extraction algorithm," Computerized Medical Imaging and Graphics, Vol. 32, No. 7, pp.566-579, 2008.

[15] A.Tenenhaus, A.Nkengne, J.F.Horn, C.Serruys, A.Giron, B.Fertil et al., "Detection of melanoma from dermoscopic images of naevi acquired under uncontrolled conditions," Skin Research and Technology, Vol. 16, pp.85-97, 2010.

[16] L.Zhao, S.Jiuai, S.Lyndon, S.Melvyn, W.Robert, "Distribution quantification on dermoscopy images for computer-assisted diagnosis of cutaneous melanomas," Medical & biological engineering & computing, Vol. 50, No. 5, pp.503-513, 2012.

[17] H.Iyatomi, H.Oka, M.E.Celebi, K.Ogawa, G.Argenziano, H.P.Soyer, H.Koga, T.Saida et al., "Comuter-based classification of dermoscopy images of melanocytic lesions on acral volar skin," Journal of Investigative Dermatology, Vol. 128, pp.2049-2054, 2008.

[18] J.Shing and R.Jang, "ANFIS : adaptive-network-based fuzzy inference system," IEEE Trans. on Systems Man and Cybernetics, Vol. 22, No. 3, pp.665-685, 1993.

[19] H.Iyatomi and M.Hagiwara, "Adaptive fuzzy inference neural network," Pattern Recognition, Vol. 32, No. 10, pp.2049-2057, 2004.

[20] H.Iyatomi, H.Oka, M.Sato, A.Miyake, M.Kimoto, J.Yamagami, S.Kobayashi, A.Tanikawa, et al., "Quantitative assessment of tumor extraction from dermoscopy images and evaluation of computer-based extraction methods for an automatic melanoma diagnostic system," Melanoma Research, Vol. 16, No. 2, pp.183-190, 2006.

[21] C.Cortes and V.Vapnik, "Support-vector networks," Machine Learning, Vol. 20, No. 3, pp.273-297, 1995.

[22] I.Guyon, J.Weston, S.Barnhill, V.Vapnik, "Gene selection for cancer classification using support vector machines," Machine Learning, Vol. 46, No. 1-3, pp.389-422, 2002.